

Effect of the Surface on the Electron Quantum Size Levels and Electron g -Factor in Spherical Semiconductor Nanocrystals

A.V. Rodina*

Institute for Solid State Physics, TU Berlin, D-10623 Berlin, Germany

Al. L. Efros

Naval Research Laboratory, Washington, DC 20375, USA

A. Yu. Alekseev

*Institute of Theoretical Physics, Uppsala University, S-75108, Uppsala, Sweden
and Department of Mathematics, University of Geneva, 1211 Geneva, Switzerland*

(Dated: November 4, 2018)

The structure of the electron quantum size levels in spherical nanocrystals is studied in the framework of an eight-band effective mass model at zero and weak magnetic fields. The effect of the nanocrystal surface is modeled through the boundary condition imposed on the envelope wave function at the surface. We show that the spin-orbit splitting of the valence band leads to the surface-induced spin-orbit splitting of the excited conduction band states and to the additional surface-induced magnetic moment for electrons in bare nanocrystals. This additional magnetic moment manifests itself in a nonzero surface contribution to the linear Zeeman splitting of all quantum size energy levels including the ground $1S$ electron state. The fitting of the size dependence of the ground state electron g factor in CdSe nanocrystals has allowed us to determine the appropriate surface parameter of the boundary conditions. The structure of the excited electron states is considered in the limits of weak and strong magnetic fields.

PACS numbers: 73.22.-f, 71.70.Ej, 78.67.Bf, 75.75.+a

I. INTRODUCTION

The modern technique of nanocrystal growth has created high optical quality nanocrystals with narrow size distribution^{1,2} that can be also chemically doped.³ This allows one to study the level structure of the nanocrystals using interband optical spectroscopy,^{4,5,6} tunneling spectroscopy,^{7,8} and the far-infrared intraband spectroscopy.^{3,9} Important additional information about the origin of these levels and their symmetry could be obtained by using optical magnetospectroscopy of the intraband and interband transitions and tunnelling magnetospectroscopy, as was done many years ago in the case of atoms, hydrogenlike shallow defects and excitons. There is the other group of experiments, such as magneto circular dichroism,¹⁰ spin-flip Raman scattering,¹¹ time dependent Faraday rotation,^{12,13} EPR and ODMR measurements,^{14,15,16} and magneto-photoluminescence,¹⁷ where the magnetic field is an essential component of the experimental technique. Interpretation of all these experiments requires the knowledge of electron and hole energy spectra in magnetic fields.

A wide class of semiconductor materials can be prepared in nanocrystal form. In most cases they have a spherical shape and can be bare semiconductor nanocrystals or onion type heterostructure nanocrystals composed of an inner semiconductor core coated with several spherical shells of different semiconductors.^{18,19,20} Technology allows one to vary the radius of the nanocrystal core from 10–40 Å in a controlled manner. The energy spec-

tra of the NCs are formed by the discrete quantum size levels (QSLs). The QSLs of the confined electrons in the conduction band are characterized by the value of the orbital momentum l and the total angular momentum $j = l \pm 1/2$, similar to the bound electron states in atoms²¹. In a zero magnetic field, the levels are degenerate with respect to the projection of the total momentum j .

The spectra of the nanocrystals in an external magnetic field H is well described as an atomic Zeeman effect. A diamagnetic H^2 contribution to the spectra could be neglected because the nanocrystal radius, a , is considerably smaller than the magnetic length, $L = \sqrt{e\hbar/cH}$, where e is the absolute value of a free electron charge, c is the speed of light. In a reasonable magnetic field $H < 10$ T the diamagnetic contribution to the QSLs $\sim (a/L)^4 \ll 1$. However, the effect of the external magnetic field on the electron QSLs depends on the zero field spin-orbit splitting, Δ_c , of the levels with different $j = l \pm 1/2$ (One can find a description of the similar effect for atoms in Ref. 21). If Δ_c is larger than the Zeeman energy, the weak magnetic field splits the electron levels:

$$\Delta E_j^\pm = \mu_B g_j^\pm m H, \quad m = -j, -j+1, \dots, j, \quad (1)$$

where $\mu_B = e\hbar/2m_0c$ is the Bohr magneton, m_0 is the free electron mass, m is the projection of the total momentum on the magnetic field direction and g_j^\pm is the effective g -factor of the corresponding state, that is an analog of the *Landé factor* for atoms. If Δ_c is small, the Zeeman splitting can be described as the sum of the

spin and orbital contributions:

$$\Delta E_l = \mu_B g_s s_z H + \mu_B g_l l_z H, \quad (2)$$

where $s_z = \pm 1/2$ and $l_z = -l, -l+1, \dots, l$ are the electron spin and angular momentum projections on a magnetic field direction correspondingly, and g_s and g_l are the spin and orbital g -factors of the electron in the corresponding state. In bare nanocrystals made of semiconductors with a simple parabolic conduction band g_s is equal to the bulk electron effective g -factor g_c and $g_l = m_0/m_c$, where m_c is the bulk electron effective mass.

Spin-flip Raman scattering studies of CdS nanocrystals,¹¹ however, have demonstrated the dependence of the ground 1S electron state g_s on the excitation energy, and thus on the energy of the electron state. The variation of g_s with energy can be connected with the energy dependence of the bulk electron g -factor.¹¹ The eight band Kane model, that is used to describe the electron energy spectra in most direct gap semiconductors, gives the following dependence of the electron g -factor $g_c(E)$ on its energy, E :^{22,23}

$$g_c(E) = g^* - \frac{2E_p}{3} \frac{\Delta}{(E_g + E)(E_g + \Delta + E)}. \quad (3)$$

Here E_g is the band gap energy, Δ is the spin-orbit splitting of the top of the valence band, E_p is the energetic Kane parameter, and $g^* = g_0 + \Delta g$, where $g_0 = 2$ is the free electron g -factor and $|\Delta g| \ll 1$ is the contribution of remote bands to the bulk electron g factor. The second term in Eq. (3) describes the negative contribution of the valence band (with $\Delta > 0$) into the electron g -factor. It decreases with increasing the energy of QSLs caused by the reduction of the nanocrystals size. Thus, the energy dependence of $g_c(E)$ in Eq. (3) is conducive to the size dependence of g_s in Eq. (2), that has been measured recently in bare and core-shell CdSe nanocrystals.¹³

The size dependence of g_s for the ground 1S electron state in the spherical heterostructure has been calculated in Ref. 24 within the eight band Kane model. It has been shown that in a spherical heterostructure formed by two semiconductors, A and B , g_s is the sum of the weighted volume contributions of each material and the interface contributions: $g_s = \overline{g_s(A)} + \overline{g_s(B)} + g_{AB}$. The interface term, g_{AB} , is proportional to the square of the conduction band component of the wave function, f_c , at the A/B heterointerface. This calculation shows clearly that g_s is very sensitive to the value of the wave function at the heterointerface and to its leakage under the barrier and thus to the boundary conditions (BCs) imposed on the wave function at the heterointerface. In Ref. 24 the size dependence of the electron g -factor is calculated using standard BCs that assumes a continuity of f_c at the interface. This leads to the vanishing of the interface term, g_{AB} , in the bare semiconductor nanocrystals, that are modeled by the infinite potential barrier in the layer B because the standard BC at the surface in this case is $f_c = 0$.

However, the standard BCs are not always justified even for infinite potential barriers (see for example Refs. 25,26). In general, the wave function f_c does not vanish at the surface of bare semiconductor nanocrystals and satisfies the general boundary conditions that are the characteristics of the particular surface.^{25,26} The effect of a semiconductor surface on the light absorption in indirect band semiconductor nanocrystals has been studied in Ref. 25 and was found to be significant.

In this paper we study the effect of the general boundary conditions on the QSLs of an electron in zero and weak external magnetic fields. We show that there is an additional surface-induced spin-orbit term for the electron states whose magnitude is proportional to $\Delta |f_c(a)|^2 a^3$. This surface-induced spin-orbit interaction leads the additional magnetic moment of the electrons in an external magnetic field in analogy with the additional relativistic magnetic moment of the electrons in atoms.^{27,28} This is conducive to the nonzero surface contribution to the electron g factor that controls the linear Zeeman splitting of the QSLs. The fitting of the experimental size dependence of the electron g factor in the ground state¹³ has allowed us to determine the appropriate parameter of the general boundary conditions for bare CdSe nanocrystals. The spectra of excited electron states has been considered in the two limits of the relation between the zero field spin-orbit splitting and the electron energy in magnetic field similar to consideration conducted for atoms.²¹

The paper is organized in the following way: In Sec. II we describe the eight-band Hamiltonians that include the external magnetic field effects. In Sec. III we derive the general boundary conditions for the conduction band component of the envelope function at the abrupt surface (see Sec. III A) and analyze the surface effect on the electron QSLs in a zero magnetic field (see Sec. III B). The effect of the weak external magnetic field on the electron QSLs is considered in Sec. IV. The size dependence of the electron ground state g factor in bare CdSe nanocrystals has been calculated and the value of the surface boundary parameter has been determined by fitting experimental data in Sec. IV B. The symmetry of the electron excited states in an external magnetic field is studied in the low and strong magnetic field regimes (see Sec. IV C). The results are summarized and discussed in Sec. V.

II. EFFECT OF A WEAK MAGNETIC FIELD ON THE QSLs WITHIN THE EIGHT-BAND MODEL: PERTURBATION APPROACH

A. The eight band model

The energy band structure of the cubic semiconductors near the center of the first Brillouin zone can be well described within the eight-band $\mathbf{k} \cdot \mathbf{p}$ model.^{29,30,31} In the homogenous semiconductor, the full wave function

can be presented as the expansion:³⁰

$$\begin{aligned} \Phi(\mathbf{r}) = & \sum_{\mu=\pm 1/2} \Psi_{\mu}^c(\mathbf{r})|S\rangle u_{\mu} + \\ & \sum_{\mu=\pm 1/2} \sum_{\alpha=x,y,z} \Psi_{\alpha\mu}^v(\mathbf{r})|R_{\alpha}\rangle u_{\mu}, \end{aligned} \quad (4)$$

where $u_{1/2}$ and $u_{-1/2}$ are the eigenfunctions of the spin operator $\hat{S} = 1/2\hat{\sigma}$, where $\hat{\sigma} = \{\hat{\sigma}_x, \hat{\sigma}_y, \hat{\sigma}_z\}$ are the Pauli matrices, $|S\rangle$ is the Bloch function of the conduction band edge at the Γ -point of Brillouin zone representing the eigenfunction of internal momentum $I = 0$, and $|R_x\rangle = |X\rangle$, $|R_y\rangle = |Y\rangle$, $|R_z\rangle = |Z\rangle$ are the Bloch functions of the valence band edge at the Γ -point of Brillouin zone. The combination of these functions: $1/\sqrt{2}(|R_x\rangle \pm i|R_y\rangle)$ and $|R_z\rangle$ are the eigenfunctions of the internal momentum $I = 1$ with projections ± 1 and 0 on the z axis respectively (see Refs. 30,32). The smooth functions $\Psi_{\pm 1/2}^c(\mathbf{r})$ are the components of the conduction band spinor envelope function $\Psi^c = \begin{pmatrix} \Psi_{1/2}^c \\ \Psi_{-1/2}^c \end{pmatrix}$, and $\Psi_{x\pm 1/2}^v(\mathbf{r})$, $\Psi_{y\pm 1/2}^v(\mathbf{r})$, $\Psi_{z\pm 1/2}^v(\mathbf{r})$ are the x, y, z components of the valence band spinor envelope vector $\Psi^v = \begin{pmatrix} \Psi_{1/2}^v \\ \Psi_{-1/2}^v \end{pmatrix} = \left\{ \begin{pmatrix} \Psi_{x1/2}^v \\ \Psi_{x-1/2}^v \end{pmatrix}, \begin{pmatrix} \Psi_{y1/2}^v \\ \Psi_{y-1/2}^v \end{pmatrix}, \begin{pmatrix} \Psi_{z1/2}^v \\ \Psi_{z-1/2}^v \end{pmatrix} \right\}$. In the presence of external magnetic field the eight-component envelope function $\Psi(\mathbf{r}) \equiv \{\Psi^c(\mathbf{r}), \Psi^v(\mathbf{r})\}$ is the solution of the Schrödinger equation²⁹

$$\begin{aligned} \hat{H}(\hat{\mathbf{k}}) \begin{pmatrix} \Psi^c \\ \Psi^v \end{pmatrix} &= E \begin{pmatrix} \Psi^c \\ \Psi^v \end{pmatrix}, \\ \hat{H}(\hat{\mathbf{k}}) &= \begin{pmatrix} \hat{H}^c(\hat{\mathbf{k}}) & i\hbar P \hat{U}_2 \hat{\mathbf{k}} \\ -i\hbar P \hat{U}_2 \hat{\mathbf{k}} & \hat{H}^v(\hat{\mathbf{k}}) \end{pmatrix}. \end{aligned} \quad (5)$$

Here, the energy E is measured from the bottom of the conduction band, $\hat{\mathbf{k}} = \frac{1}{\hbar} \left(\hat{\mathbf{p}} + \frac{e}{c} \mathbf{A} \right)$, where $\hat{\mathbf{p}} = -i\hbar \nabla$ is the momentum operator and $\mathbf{A} = (1/2)[\mathbf{H} \times \mathbf{r}]$ is the vector potential of the magnetic field. The 2×2 unit matrix, \hat{U}_2 , and the Pauli matrices, σ_x , σ_y and σ_z , are acting on the spinor components of the wave functions ($\mu = \pm 1/2$). $P = -i\langle S|\hat{p}_z|Z\rangle/m_0$ is the Kane matrix element describing the coupling of the conduction and valence bands (The Kane energy parameter: $E_p = 2m_0P^2$, was introduced in Eq. (3), respectively). The off-diagonal matrix element in Eq. (5) acts on the Ψ^v as a scalar product $\sim \hat{\mathbf{k}}\Psi^v \equiv \hat{k}_x\Psi_x^v + \hat{k}_y\Psi_y^v + \hat{k}_z\Psi_z^v$. The conduction band part of the Hamiltonian, \hat{H}^c , acting on the spinor function Ψ^c has the form:

$$\hat{H}^c(\hat{\mathbf{k}}) = \frac{\alpha\hbar^2}{2m_0} \hat{U}_2 \hat{k}^2 + \frac{1}{2}g^* \mu_B (\hat{\sigma} \mathbf{H}), \quad (6)$$

where g^* is defined in Eq. (3), and α takes into account the contribution of remote bands to the energy-dependent electron effective mass, $m_c(E)$. In cubic and

zinc-blende semiconductors this dependence has the following form:

$$\frac{m_0}{m_c(E)} = \alpha + \frac{E_p}{3} \left[\frac{2}{E_g + E} + \frac{1}{E_g + E + \Delta} \right]. \quad (7)$$

In this paper we focus only on the electron QSLs with energies $0 < E < E_g$. This allows us to neglect hereafter the k^2 terms in the valence band part of the Hamiltonian, \hat{H}^v , and to present it in the spherical approximation as:^{30,32}

$$\begin{aligned} \hat{H}^v(\hat{\mathbf{k}}) = & - \left(E_g + \frac{1}{3}\Delta + (1 + 3\kappa)(\hat{\mathbf{I}}\mathbf{H}) \right) \hat{U}_2 \\ & + \frac{1}{3}\Delta(\hat{\mathbf{I}}\hat{\sigma}) + \frac{1}{2}\mu_B g_0(\hat{\sigma}\mathbf{H}). \end{aligned} \quad (8)$$

Here, the Hamiltonian \hat{H}^v should be considered as the 2×2 matrix acting on the spinor vector Ψ^v rather than the 6×6 matrix Hamiltonian acting on the six component wave function as in Ref. 32. Correspondingly, $\hat{\mathbf{I}} = \{\hat{I}_x, \hat{I}_y, \hat{I}_z\}$ in Eq. (8) is the vector operator. It is straightforward to show that in this representation $(\hat{\mathbf{I}}\mathbf{T})\Psi^v = -i[\mathbf{T} \times \Psi^v]$, where \mathbf{T} is an arbitrary vector. The terms proportional to Δ in Hamiltonian (8) describe the effect of the spin-orbit coupling and $\kappa = \kappa^L - E_p/6E_g$,²⁹ where κ^L is the magnetic Luttinger parameter.³² One can find that $\kappa = -2/3$ from the relation:^{29,33} $\kappa^L = (-2 - \gamma_1^L + 2\gamma_2^L + 3\gamma_3^L)/3$, where the effective mass Luttinger parameters,³² $\gamma_{1,2,3}^L$, can be presented as: $\gamma_1^L \approx E_p/3E_g$ and $\gamma_2^L \approx \gamma_3^L \approx E_p/6E_g$ in the approximation used above.²⁹

B. Linear Zeeman effect as a perturbation

Following the perturbation approach developed in Ref. 24, we present the Hamiltonian (5) as:

$$\hat{H}_{PB}(\hat{\mathbf{k}}) = \hat{H}^0(\hat{\mathbf{p}}) + \hat{H}'(\hat{\mathbf{p}}, \mathbf{H}), \quad (9)$$

where the Hamiltonian \hat{H}^0 describes the electron states in zero magnetic field:

$$\hat{H}^0(\hat{\mathbf{p}}) = \begin{pmatrix} \frac{\alpha}{2m_0} \hat{U}_2 \hat{p}^2 & iP \hat{U}_2 \hat{\mathbf{p}} \\ -iP \hat{U}_2 \hat{\mathbf{p}} & \frac{1}{3}\Delta(\hat{\mathbf{I}}\hat{\sigma}) - (E_g + \frac{1}{3}\Delta) \hat{U}_2 \end{pmatrix}, \quad (10)$$

and the Hamiltonians \hat{H}' describes the effect of a weak external magnetic field. Linear in the magnetic field terms of $\hat{H}'(\hat{\mathbf{p}}, \mathbf{H})$ can be written:

$$\hat{H}'(\hat{\mathbf{p}}, H) = \mu_B H \hat{G} + \frac{e}{c} \{ \mathbf{A}, \hat{\mathbf{V}} \} \equiv \mu_B H (\hat{G} + \hat{G}'), \quad (11)$$

where $\{a, b\} = 1/2(ab + ba)$ denotes an anticommutator and $\hat{\mathbf{V}} = \partial \hat{H}^0(\mathbf{p}) / \partial \mathbf{p}$ is the envelope velocity operator. The operators \hat{G} and \hat{G}' are defined as:

$$\hat{G} = \begin{pmatrix} \frac{1}{2}g^*(\hat{\sigma}\mathbf{n}) & 0 \\ 0 & (\hat{\mathbf{I}}\mathbf{n})\hat{U}_2 + \frac{1}{2}g_0(\hat{\sigma}\mathbf{n}) \end{pmatrix}, \quad (12)$$

$$\hat{G}' = \begin{pmatrix} \alpha(\hat{\mathbf{L}}\mathbf{n}) & iP\frac{m_0}{\hbar}[\mathbf{n} \times \mathbf{r}] \\ -iP\frac{m_0}{\hbar}[\mathbf{n} \times \mathbf{r}] & 0 \end{pmatrix} \hat{U}_2, \quad (13)$$

where $\mathbf{n} = \mathbf{H}/H$ is the unit vector directed along the external magnetic field, and $\hat{\mathbf{L}} = \frac{1}{\hbar}[\mathbf{r} \times \hat{\mathbf{p}}]$ is the envelope angular momentum operator.

Generally, the calculation of the linear Zeeman effect for the carriers confined in a 3D external potential of arbitrary shape is a straightforward theoretical problem. The same procedure is used for an impurity potential and for a zero dimensional quantum dot of an arbitrary shape. Using the unperturbed Hamiltonian \hat{H}^0 one has to find first the energy levels E_λ and the corresponding eigen functions $\Psi_\lambda = \{\Psi^c, \Psi^v\}$ of the carrier in the external confining potential. Then, the effect of the magnetic field can be found perturbatively:

$$\Delta E_\lambda = \mu_B H \left[\langle \Psi_\lambda | \hat{G}' | \Psi_\lambda \rangle + \langle \Psi_\lambda | \hat{G}' | \Psi_\lambda \rangle \right]. \quad (14)$$

where the wave functions should be normalized $\langle \Psi_\lambda | \Psi_\lambda \rangle = 1$. Substituting Ψ_λ into this expression we obtain:

$$\Delta E_\lambda = \Delta E_c + \Delta E_v + \Delta E_{coup}, \quad (15)$$

where the contribution of the valence and conduction bands to Zeeman effect ΔE_c and ΔE_v correspondingly are:

$$\frac{\Delta E_c}{\mu_B H} = \frac{1}{2} \langle \Psi^c | g^*(\hat{\boldsymbol{\sigma}}\mathbf{n}) | \Psi^c \rangle + \langle \Psi_\mu^c | \alpha(\hat{\mathbf{L}}\mathbf{n}) | \Psi_\mu^c \rangle, \quad (16)$$

$$\frac{\Delta E_v}{\mu_B H} = \frac{1}{2} \langle \Psi^v | g_0(\hat{\boldsymbol{\sigma}}\mathbf{n}) | \Psi^v \rangle + \langle \Psi_\mu^v | (\hat{\mathbf{I}}\mathbf{n}) | \Psi_\mu^v \rangle, \quad (17)$$

and the coupling correction is given by

$$\begin{aligned} \frac{\Delta E_{coup}}{\mu_B H} &= \left\langle \Psi^c \left| i \frac{m_0 P}{\hbar} \hat{U}_2 [\mathbf{n} \times \mathbf{r}] \right| \Psi^v \right\rangle \\ &+ \left\langle \Psi^c \left| i \frac{m_0 P}{\hbar} \hat{U}_2 [\mathbf{n} \times \mathbf{r}] \right| \Psi^v \right\rangle^*. \end{aligned} \quad (18)$$

In principle, this straightforward approach allows us to find the linear Zeeman splitting of the energy levels in any arbitrarily shaped hetero-nanostructure. However, the calculations of the zero field wave functions Ψ_λ for arbitrary shape heterostructure is a rather cumbersome procedure and, consequently, the Zeeman splitting calculation that uses these wave functions is very complicated. In the present paper, from hereafter, only spherical semiconductor nanocrystals are considered. The high symmetry of these quantum dots allow us to calculate the Zeeman splitting of the QSLs.

III. ENERGY LEVELS OF THE ELECTRON CONFINED IN BARE SPHERICAL NANOCRYSTALS

A. General boundary conditions for the envelope wave functions

We will consider bare semiconductor nanocrystals which surface can be modeled by an impenetrable bar-

rier. To find unperturbed envelope wave functions that are described by the Hamiltonians of Eq. (10) in the bulk region one should impose an appropriate boundary conditions on these functions at the nanocrystal surface. For the impenetrable barrier the general boundary conditions (GBCs) have been shown in Ref. 26 to guarantee the vanishing of the normal to the surface component of the envelope flux density matrix. In a spherical nanocrystal the normal envelope flux density matrix, $J_\tau^{\lambda\eta}(\mathbf{r})$, should vanish at any point of the nanocrystals surface:

$$\begin{aligned} J_\tau^{\lambda\eta}(\mathbf{r})|_{r=a} &\equiv \boldsymbol{\tau} \cdot \mathbf{J}^{\lambda\beta}|_{r=a} = \\ \frac{1}{2} \left[\left(\Psi_\lambda, \boldsymbol{\tau} \cdot \hat{\mathbf{V}} \Psi_\eta \right) + \left(\boldsymbol{\tau} \cdot \hat{\mathbf{V}} \Psi_\lambda, \Psi_\eta \right) \right] \Big|_{r=a} &= 0, \end{aligned} \quad (19)$$

where a is the nanocrystal radius and $\boldsymbol{\tau} = \mathbf{r}/r$ (in spherical coordinates \mathbf{r} is defined as $\mathbf{r} \equiv (r, \Theta, \varphi)$). This general requirement of Eq. (19) should be satisfied for two arbitrarily chosen eigenfunctions Ψ_λ and Ψ_η of the Hamiltonian \hat{H}^0 defined in Eq. (10) with energies E_λ and E_η , respectively. Substituting the explicit expressions for the normal components of the envelope velocities $\boldsymbol{\tau} \cdot \hat{\mathbf{V}} = \boldsymbol{\tau} \cdot \partial \hat{H}^0 / \partial \mathbf{p}$ into Eq. (19) one obtains:

$$\begin{aligned} J_\tau^{\lambda\eta}(\mathbf{r})|_{r=a} &= \frac{i\hbar}{2m_0} \left[\alpha (\Psi_\eta^c \boldsymbol{\tau} \cdot \nabla \Psi_\lambda^{c*} - \Psi_\lambda^{c*} \boldsymbol{\tau} \cdot \nabla \Psi_\eta^c) \right. \\ &\left. + \frac{2m_0 P}{\hbar} (\boldsymbol{\tau} \cdot \Psi_\eta^v \Psi_\lambda^{c*} - \boldsymbol{\tau} \cdot \Psi_\lambda^{v*} \Psi_\eta^c) \right] \Big|_{r=a} = 0. \end{aligned} \quad (20)$$

Using equation $\hat{H}^0 \Psi = E \Psi$ one can express the components of the spin vector Ψ^v through $\nabla \Psi^c$:

$$\begin{aligned} \Psi^v &= \frac{\hbar}{2m_0 P} \left(\alpha - \frac{m_0}{m_c(E)} \right) \nabla \Psi^c \\ &+ \frac{i\hbar}{4m_0 P} (g_c(E) - g^*) [\hat{\boldsymbol{\sigma}} \times \nabla \Psi^c], \end{aligned} \quad (21)$$

where the energy dependent electron effective mass $m_c(E)$ and g -factor $g_c(E)$ are defined in Eqs. (7) and (3) respectively. The normal projection $(\boldsymbol{\tau} \Psi^v)$ can then be written:

$$\begin{aligned} \boldsymbol{\tau} \Psi^v(\mathbf{r}) &= \frac{\hbar}{2m_0 P} \left(\alpha - \frac{m_0}{m_c(E)} \right) \frac{\partial \Psi^c}{\partial r} \\ &- \frac{\hbar}{4m_0 P r} \Delta g(E) (\hat{\boldsymbol{\sigma}} \hat{\mathbf{L}}) \Psi^c, \end{aligned} \quad (22)$$

where $\Delta g(E) = g^* - g_c(E)$. Substituting Eq. (22) into Eq. (20) one obtains the general requirement for the conduction band component of the envelope wave function at the NC surface:

$$J_\tau^\lambda \eta(a) = \frac{i\hbar}{2m_0} \left[\left(\frac{m_0}{m(E_\lambda)} \Psi_\eta^c \frac{\partial \Psi_\lambda^{c*}}{\partial r} - \frac{m_0}{m(E_\eta)} \Psi_\lambda^{c*} \frac{\partial \Psi_\eta^c}{\partial r} \right) + \frac{1}{2r} \left(\Psi_\eta^c \Delta g(E_\lambda) (\hat{\sigma} \hat{L}) \Psi_\lambda^{c*} - \Psi_\lambda^{c*} \Delta g(E_\eta) (\hat{\sigma} \hat{L}) \Psi_\eta^c \right) \right] \Big|_{r=a} = 0. \quad (23)$$

Equation (23) must be fulfilled at each point of the surface. It is satisfied for all arbitrary chosen energy states λ and η if and only if the boundary conditions for Ψ_λ^c as well as for Ψ_η^c are given by:

$$\Psi^c(r = a, \Theta, \varphi) = Ta_0 \left(\frac{m_0}{m_c(E)} \frac{\partial \Psi^c(r, \Theta, \varphi)}{\partial r} + \frac{1}{2r} \Delta g(E) (\hat{\sigma} \hat{L}) \Psi^c(r, \Theta, \varphi) \right) \Big|_{r=a}, \quad (24)$$

where T is a real number constant independent of E and a_0 is the lattice constant. We assume that the surface of the nanocrystal also possesses the spherical symmetry and is characterized by the same BCs at any point of the surface. In this case parameter T in the GBCs of Eq. (24) is independent of angles Θ and φ .

B. Electron energy levels: the surface induced spin-orbit splitting

Let us consider the effect of the GBCs of Eq. (24) on the electron QSLs in the absence of a magnetic field. Using Eq. (21) that expresses the valence band component Ψ^v of the wave function through its conduction band component Ψ^c one can derive the bulk Schrödinger equation describing Ψ^c inside a semiconductor nanocrystal:

$$-\frac{\hbar^2}{2m_c(E)} \hat{U}_2 \nabla^2 \Psi^c(\mathbf{r}) = E \Psi^c(\mathbf{r}). \quad (25)$$

One can see that each spin component of Ψ^c is a solution of the standard bulk Schrödinger equation with the energy dependent effective mass $m_c(E)$. Equation (25) does not contain a spin-orbit term and its solution can always be presented as $f_l(r) Y_{l,l_z}(\Theta, \varphi)$, where l and l_z are the angular momentum and angular momentum projection, correspondingly, $Y_{l,l_z}(\Theta, \varphi)$ are the spherical harmonics, and the radial function $f_l(r)$ satisfies to the following equation:

$$-\frac{\hbar^2}{2m_c(E)} \Delta_l f_l(r) = E f_l(r), \quad (26)$$

$$\Delta_l = \frac{\partial^2}{\partial r^2} + \frac{2}{r} \frac{\partial}{\partial r} - \frac{l(l+1)}{r^2}.$$

At the same time the GBCs of Eq. (24) mixes two electron spin sublevels, and all electron states are characterized now by the total angular momentum: $\mathbf{j} = \mathbf{L} + \mathbf{S}$.

As a result Ψ^c is an eigen spinor of the operator of the total angular momentum:

$$\Psi^c = f_l^\pm(r) \Omega_{j,l,m}(\Theta, \varphi), \quad (27)$$

where $\Omega_{j,l,m}(\Theta, \varphi)$ are the spherical spinors, j and m are the total angular momentum and its projection respectively, and l is the angular momentum of the electron state. The two radial functions f_l^\pm describe the two electron states with $j = l \pm 1/2$ (note that the states described by f_l^- exist only for $l \geq 1$). We use the definition of the spherical spinors as in Ref. 34

$$\Omega_{j,l,m} = \begin{pmatrix} C_{1/2,1/2;l,m-1/2}^{j,m} Y_{l,m-1/2} \\ C_{1/2,-1/2;l,m+1/2}^{j,m} Y_{l,m+1/2} \end{pmatrix}, \quad (28)$$

where $j = l \pm 1/2$ and $C_{j_1, m_1; j_2, m_2}^{j, m}$ are the Clebsch-Gordan coefficients. Substituting Eq. (27) into Eq. (24) one can write the general boundary condition for the radial wave functions $f_l^\pm(r)$:

$$f_l^\pm(a) = Ta_0 \left[\frac{m_0}{m_c(E)} f_l^{\pm\prime}(a) + \delta k_l^\pm f_l^\pm(a) \right], \quad (29)$$

where

$$\delta k_l^+ = \frac{l}{2a} \Delta g(E), \quad l = 0, 1, 2, \dots, \quad (30)$$

for the states with $j = l + 1/2$ and

$$\delta k_l^- = -\frac{l+1}{2a} \Delta g(E), \quad l = 1, 2, 3, \dots, \quad (31)$$

for the states with $j = l - 1/2$. The conventionally used standard BCs for the impenetrable barrier assumes vanishing of the wave function Ψ^c at the nanocrystal surface, and thus correspond to $Ta_0 = 0$. In general, however, the conduction band component of the wave function does not vanish at the surface. Furthermore, it has been shown in Ref.26 that the boundary condition with $Ta_0 = 0$ is incorrect in cases where interband coupling is important. The appropriate value of Ta_0 should be determined from the fitting to the experimental data.

The solutions of Eq. (26) can be written as $f_l^\pm(r) = (C_l^\pm / a^{3/2}) j_l(\phi_{l,n}^\pm r/a)$, where j_l are spherical Bessel functions, C_l^\pm is the normalization constant determined by the condition $\int (|\Psi^c|^2 + |\Psi^v|^2) dV = 1$, and $\phi_{l,n}^\pm$ is connected with the energy, E , of the electron level: $E = \hbar^2 \phi_{l,n}^{\pm 2} / 2m_c(E) a^2$. An equation that determined $\phi_{l,n}^\pm$ is

obtained by substitution of $f_l^\pm(r)$ into the BCs of Eq. (29):

$$j_l(\phi_{l,n}^\pm) [1 - \delta k_l^\pm T a_0] = \quad (32)$$

$$\frac{T a_0}{a} \frac{m_0}{m_c(E)} \phi_{l,n}^\pm \left[\frac{l}{2l+1} j_{l-1}(\phi_{l,n}) - \frac{l+1}{2l+1} j_{l+1}(\phi_{l,n}) \right].$$

The n^{th} solution of this equation defines the energy of the n^{th} electron level with the angular momentum l and the total angular momentum $j = l \pm 1/2$. In the case of the standard BCs $T a_0 = 0$, and the solution $\phi_{l,n}^\pm$ is the n -th zero $\phi_{l,n}^0$ of the spherical Bessel functions j_l . The general BCs with $T a_0 \neq 0$ takes into account the effect of the surface on the electron energy levels that is important in small nanocrystals. In large nanocrystals satisfying the condition $a \gg |T a_0|(m_0/m_c)$, the solutions $\phi_{l,n}^\pm$ are close to $\phi_{l,n}^0$ and the effect of the surface on the confined electron states is negligible.

The electron states with $j = l + 1/2$ and $j = l - 1/2$ have different energies for $l \geq 1$ as a result of the general BCs of Eq. (29). This difference describes the surface induced spin-orbit splitting of the excited states: $\Delta_c = E_{l+1/2} - E_{l-1/2}$. It can be shown that Δ_c is positive if the spin-orbit splitting of the valence band $\Delta > 0$.

Figure 1 shows the effect of the general BCs on the energy of the ground $1S$ ($l = 0$) and the first excited $1P$ ($l = 1$) electron states in bare CdSe nanocrystals. The surface induced spin-orbit interaction splits the last state into two states with the total angular momentum $j = 3/2$ ($P_{3/2}$ state) and $j = 1/2$ ($P_{1/2}$ state) and the size dependence of this splitting $\Delta_c = E(1P_{3/2}) - E(1P_{1/2})$ is shown in Fig. 1(b). The calculations have been performed for the following bulk parameters of CdSe: $E_p = 19.0$ eV and $m_c(0) = 0.116 m_0$ from Ref. 35, $E_g = 1.839$ eV, $\Delta = 0.42$ meV, and $g_c(0) = 0.68$ from Ref. 36, that result in $\alpha = -1.07$ and $g^* = 1.96$. One can see that even a small surface parameter introduced by the GBCs, $|T a_0| = 0.6 \text{ \AA}$, significantly affects both ground and excited states in small nanocrystals. The positive (negative) value of the surface parameter $T a_0 > 0$ ($T a_0 < 0$) increases (decreases) the energy of all states in comparison with $T a_0 = 0$. The relative order of the $P_{3/2}$ and $P_{1/2}$ states with the total momentum $j = 3/2$ and $j = 1/2$ always coincides with the relative order of the valence band subbands characterized by the same total momentum. The value of the spin-orbit splitting, Δ_c , however, remains for all excited states much smaller than the averaged energy $E_l = (l E_{l-1/2} + (l+1) E_{l+1/2}) / (2l+1)$ of the level with the orbital momentum l .

If $|\delta k_l^\pm T a_0| \ll 1$, the averaged energies E_l and corresponding wave numbers $\phi_{l,n}$ can be found from the simplified BCs given by Eqs. (29, 32) with $\delta k_l^\pm = 0$. The energy corrections ΔE_l^\pm coming from the small $\delta k_l^\pm \neq 0$ can be found perturbatively. In the Appendix we obtain the following energy corrections:

$$\Delta E_l^\pm = \frac{\hbar^2}{2m_0} |f_l^\pm(a)|^2 a^2 \delta k_l^\pm =$$

$$\frac{\hbar^2}{4m_0} \int \left(\Delta g(E) \Psi^{c*}(\hat{\sigma} \hat{L}) \Psi^c \right) \frac{1}{r} dS, \quad (33)$$

where $dS = r^2 \sin(\Theta) d\Theta d\varphi$. Note that although $\phi_{l,n}^+ = \phi_{l,n}^- = \phi_{l,n}$, the normalization constants $C_l^+ \neq C_l^-$. However, in the considered approximation they can be replaced with high accuracy by the averaged constant $C_l = C_l^+ = C_l^-$ that is determined by the approximate normalization condition:

$$\int_0^a |f_l|^2 r^2 dr + \int_0^a |\Phi_l|^2 r^2 dr = 1, \quad (34)$$

$$|\Phi_l|^2 = \frac{\hbar^2}{2m_0 E_p} \left(\alpha - \frac{m_0}{m_c(E)} \right)^2 \left(|f_l'|^2 + \frac{l(l+1)}{r^2} |f_l|^2 \right),$$

that neglects the second term in Eq. (21). Thus, if $|\delta k_l^\pm T a_0| \ll 1$, $\Delta_c < E_l$, the energy levels of the excited states E_l^\pm with $j = l \pm 1/2$ are the eigen energies of the effective Hamiltonian \hat{H}_l :

$$\hat{H}_l \Omega_{l \pm 1/2, l, m} = E_l^\pm \Omega_{l \pm 1/2, l, m},$$

$$\hat{H}_l = E_l \hat{U}_2 + \frac{1}{2l+1} \Delta_c(E_l) (\hat{L} \hat{\sigma}) \quad (35)$$

where the energy dependent spin-orbit splitting $\Delta_c(E_l)$ is given by

$$\Delta_c(E_l) = \left(l + \frac{1}{2} \right) \frac{\hbar^2}{2m_0 a^2} \Sigma_{sur}(E_l), \quad (36)$$

$$\Sigma_{sur}(E_l) = \Delta g(E_l) a^3 |f_l(a)|^2 = \Delta g(E_l) C_l^2 j_l^2(\phi_{l,n}). \quad (37)$$

The approximate expressions of Eqs. (36,37) describe the exact splitting $\Delta_c(E_1)$ of the $1P$ states in CdSe nanocrystals shown in Fig. 1(b) with high accuracy (the largest error in the smallest nanocrystals is about 2% for $T a_0 = -0.6 \text{ \AA}$). It is important to note here that while the matrix elements of the spin-orbit operator ($\hat{L} \hat{\sigma}$) are nonzero only for $l \geq 1$, Eq. (37) defines also the surface parameter Σ_{sur} for the $l = 0$ S symmetry states.

The dimensionless parameter Σ_{sur} is proportional to the spin-orbit splitting in the valence band Δ and to the square of the wave function at the surface. It describes the surface-induced spin-orbit coupling of the conduction electron QSLs in bare semiconductor nanocrystals. In bulk semiconductors the integration in Eq. (33) results in zero spin-orbit splitting of the conduction band states because it must be carried out at the remote bounding surface where the wave function is vanishing. $\Sigma_{sur} = 0$ if one assumes the vanishing of the conduction band component wave function at the surface of spherical nanocrystals. This assumption is never justified if the coupling between conduction band and valence band components is significant. Thus, the spin-orbit splitting of the electron QSLs is caused by the admixture of the valence band states near the surface.

IV. THE FINE STRUCTURE OF ELECTRON QSLs IN A MAGNETIC FIELD

A. Surface induced magnetic moment of the confined electrons

Let us consider now the energy of the electron QSLs, E_l^\pm , in a weak magnetic field. Substituting the zero field wave functions $\Psi = \{\Psi^c, \Psi^v\}$ given by Eq. (27) and (21) into Eqs. (16) and (18), we obtain for the energy correction $\Delta E \approx \Delta E_c + \Delta E_{coup}$:

$$\Delta E = \mu_B H \left[\frac{1}{2} \langle \Psi^c | g_c(E) (\hat{\boldsymbol{\sigma}} \mathbf{n}) | \Psi^c \rangle + \left\langle \Psi^c \left| \frac{m_0}{m_c(E)} (\hat{\mathbf{L}} \mathbf{n}) \right| \Psi^c \right\rangle \right] + \Delta E_{sur}, \quad (38)$$

where we neglect ΔE_v corrections of Eq. (17) as being smaller by the factor $E_l/(E_l + E_g)$. The second term of Eq. (38) describes the unexpected surface contribution to the electron magnetic energy:

$$\Delta E_{sur} = \frac{\mu_B H}{4} \int dS \frac{1}{r} \Delta g(E_l) (\Psi^{c*} [\mathbf{r} \times [\hat{\boldsymbol{\sigma}} \times \boldsymbol{\tau}] \Psi^c). \quad (39)$$

The effective Hamiltonian describing the fine structure of the electron state with the orbital momentum l in a magnetic field can be written as $\hat{H}_l + \hat{H}_H$, where \hat{H}_l is defined by Eq. (35) and the effect of a weak magnetic field is described by:

$$\hat{H}_H = \frac{1}{2} \mu_B \bar{g}_s(E_l) (\hat{\boldsymbol{\sigma}} \mathbf{H}) + \mu_B \bar{g}_l(E_l) (\hat{\mathbf{L}} \mathbf{H}) + \frac{1}{4} \mu_B \Sigma_{sur}(E_l) ([\boldsymbol{\tau} \times [\hat{\boldsymbol{\sigma}} \times \boldsymbol{\tau}] \mathbf{H}]. \quad (40)$$

Here the weighted spin \bar{g}_s and orbital \bar{g}_l g factors are given by

$$\bar{g}_s = \int_0^a g_c(E_l) r^2 dr |f_l(r)|^2, \quad (41)$$

$$\bar{g}_l = \int_0^a m_0/m_c(E_l) r^2 dr |f_l(r)|^2, \quad (42)$$

respectively. The first two terms in Eq. (40) describe the averaged volume energy of the spin $\boldsymbol{\mu}_S = -\mu_B \bar{g}_s(E_l) \mathbf{S}$ and orbital $\boldsymbol{\mu}_L = -\mu_B \bar{g}_l(E_l) \hat{\mathbf{L}}$ magnetic moments in an external magnetic field, and the last term describes the energy of the surface-induced magnetic moment $\boldsymbol{\mu}_{sur}(E_l)$ given by:

$$\boldsymbol{\mu}_{sur} = -\frac{\mu_B}{4} \Sigma_{sur}(E_l) [\boldsymbol{\tau} \times [\hat{\boldsymbol{\sigma}} \times \boldsymbol{\tau}]. \quad (43)$$

This magnetic moment arises from the surface-induced spin-orbital term of Eq. (35) which is modified by the Larmor precession of the electron in an external magnetic field. Indeed, the surface energy term $\Delta E_{sur} = -(\boldsymbol{\mu}_{sur} \mathbf{H})$ can be obtained directly by replacing $-i\nabla \rightarrow -i\nabla + (e/c\hbar)\mathbf{A}$ in the spin-orbit perturbation term

$(\hat{\mathbf{L}} \hat{\boldsymbol{\sigma}}) = -i([\mathbf{r} \times \nabla] \hat{\boldsymbol{\sigma}})$ of Eq. (35). The origin of the surface-induced electron magnetic moment is similar to those of an additional relativistic magnetic moment of the electron in atoms, and their values are derived in a similar way (see for example Refs. 21,27,28). It is necessary to note that the surface-induced magnetic moment $\boldsymbol{\mu}_{sur}$ does not vanish for the states with $l = 0$ even when it arises from the spin-orbit coupling term $(\hat{\mathbf{L}} \hat{\boldsymbol{\sigma}})$.

B. Size dependence of the ground state electron g factor

All electron states that have S symmetry are Kramers doublets that are degenerate with respect to its spin projection. The external magnetic field lifts this degeneracy and splits these states into two levels with energy:

$$E_0(H) = E_0 \pm \frac{1}{2} \mu_B g_s(E_0) H, \quad (44)$$

where the \pm signs correspond to the electron states with spins parallel and antiparallel to the magnetic field direction. The spin effective g factor can be obtained from Eq. (40) as:

$$g_s(E_0) = \bar{g}_s(E_0) + \frac{1}{3} \Sigma_{sur}. \quad (45)$$

The effective electron g factor for the S electron states in spherical heterostructures, $g_s(E_0)$, was first obtained in Ref. 24 where the standard BCs at the heterointerface were used to describe the size dependence of the electron g factor. In the case of the bare semiconductor nanocrystals the standard BC at the surface ($f_0(a) = 0$) would lead to zero surface contribution to the effective electron g factor. We have examined here the effect of the general BC of Eq. (29) on the electron effective g factor in CdSe nanocrystals. The weighted g factor of the states with S symmetry in Eq. (45) can be written:

$$\bar{g}_s(E) = g_0 + \int_0^a r^2 dr |f_l(r)|^2 (g_c(E) - g_0), \quad (46)$$

where the corrections ΔE_v of Eq. (17) to the \bar{g}_s of Eq. (41) have been added. Figure 2 shows the size dependence of the ground state electron g factor, $g_s(E_0)$, calculated using the standard BC with $|Ta_0| = 0$ and the general BC with $|Ta_0| = 0.6 \text{ \AA}$. One can see that the experimental size dependence of the electron g -factor taken from Ref. 13 is described very well by the general BC with the negative parameter $Ta_0 = -0.6$, while the use of the positive parameter brings the theoretical curve far away from the data.

The size dependence of the bulk-like energy-dependent g factor, $g_c(E_0)$, calculated with the help of Eq. (3) for $Ta_0 = 0$ is also shown in Fig. 2. One can see that the bulk g -factor g_c fails to describe the experimental data even in the largest dots. At the same time, the difference between two g_s curves calculated

with $T_{a_0} = -0.6 \text{ \AA}$ and $T_{a_0} = 0$ is not very large. This is because the general BCs affects the electron g -factor in two ways: indirectly, through the change of the zero field energy E_0 decreasing/increasing the electron g -factor, and directly, through the surface contribution $1/3\Sigma_{sur}(1S)$, that is always positive. In the case of the negative $T_{a_0} < 0$ the GBCs decreases the energy of the ground electron state decreasing the electron g -factor, and these two effects partly compensate for each other. However, the surface contribution $1/3\Sigma_{sur}(1S)$ calculated with $T_{a_0} = -0.6 \text{ \AA}$ is significant in small nanocrystals (see Fig. 3).

C. Symmetry of the confined electron excited states in an external magnetic field

The fine structure of the excited electron states in an external magnetic field is very sensitive to the relation between $\Delta_c(E_l)$ and the energy of the orbital magnetic moment $\bar{g}_l\mu_B H$. In the *low-field regime*, when the magnetic energy is smaller than the separation between the electron states with $j = l \pm 1/2$, the external magnetic field satisfying the condition $\bar{g}_l\mu_B H \ll \Delta_c$ splits the levels according to projection m of the full momentum j on the magnetic field as:

$$E_{j,m}^+ = E_l + \Delta_c(E_l)\frac{l}{2l+1} + \mu_B g_j^+(E_l) m H, \quad (47)$$

for $j = l + 1/2$ and

$$E_{j,m}^- = E_l - \Delta_c(E_l)\frac{l+1}{2l+1} + \mu_B g_j^-(E_l) m H. \quad (48)$$

for $j = l - 1/2$. The effective electron g -factors

$$g_j^+ = \frac{1}{2j}\bar{g}_s(E_l) + \frac{2j-1}{2j}\bar{g}_l(E_l) + \frac{2j+1}{8j(j+1)}\Sigma_{sur}, \quad (49)$$

$$g_j^- = \frac{-1}{2(j+1)}\bar{g}_s(E_l) + \frac{2j+3}{2(j+1)}\bar{g}_l(E_l) - \frac{2j+1}{8j(j+1)}\Sigma_{sur} \quad (50)$$

are the analogs of the Lande factors for electrons in atoms in the case of the "anomalous" Zeeman effect.²¹ The surface contributions to the electron g -factors ($\propto \Sigma_{sur}$) are similar to the relativistic corrections in Refs. 27,28.

When the zero field fine structure splitting becomes smaller than the energy of the orbital magnetic moment, the magnetic field Zeeman term mixes the states with different $j = l \pm 1/2$. In this case the projections of the spin momentum s_z and orbital momentum l_z on the direction of the magnetic field are a more convenient notation for describing the electron state fine structure. The spin-orbit term (\mathbf{LS}) and the additional surface moment ($\mu_{sur}\mathbf{H}$) may, however, mix the states with different values of the $s_z l_z$ product.

Let us consider the matrix elements of the surface magnetic moment operator μ_{sur} on the eigen-functions of one

angular momentum l . Assuming that the states with different l are not mixed, one can find:

$$\frac{r_i r_j}{r^2} Y_{l,m}(\Theta, \varphi) = \left(\frac{2l-1+2l^2}{(2l+3)(2l-1)} \delta_{ij} - \frac{2}{(2l+3)(2l-1)} \{L_i L_j\} \right) Y_{l,m}(\Theta, \varphi), \quad (51)$$

where $i, j = x, y, z$ and δ_{ij} is the Kronecker delta symbol. Substituting Eq. (51) into $(\mathbf{H}[\boldsymbol{\tau} \times [\hat{\boldsymbol{\sigma}} \times \boldsymbol{\tau}]] = (\mathbf{H}\hat{\boldsymbol{\sigma}}) - (\mathbf{H}\boldsymbol{\tau})(\boldsymbol{\tau}\hat{\boldsymbol{\sigma}})$, we rewrite the magnetic field Hamiltonian \hat{H}_H of Eq. (40) as:

$$\hat{H}_H = \mu_B g_s(E_l)(\mathbf{SH}) + \mu_B \bar{g}_l(E_l)(\mathbf{LH}) + \mu_B \Sigma_{sur}(E_l) \frac{(\mathbf{SH})\hat{L}^2 + \{(\mathbf{SL})(\mathbf{LH})\}}{(2l+3)(2l-1)}. \quad (52)$$

Here the spin electron g factor is given by

$$g_s(E_l) = \bar{g}_s(E_l) - \frac{1}{(2l+3)(2l-1)}\Sigma_{sur}(E_l). \quad (53)$$

The matrix elements of the last term in Eq. (52) are zero for $l = 0$. If $\Sigma_{sur}(E_l) \ll \bar{g}_l(E_l)$ one can neglect the off diagonal elements of the operator $\{(\mathbf{SL})(\mathbf{LH})\}$ and replace them with $(\mathbf{SH})(\mathbf{L}n)^2$. This is the case for the first excited $1P$ state in CdSe nanocrystals (for comparison, see the corresponding curves in Figs. 3 and 4). In this case the last term of Eq. (52) describes the surface contribution to the spin splitting of the electron levels that depends on the projection of the orbital momentum on the magnetic field.³⁷

In the *strong field regime* (similar to the case of the "quasi-normal" Zeeman effect or "complete" Paschen-Back effect for the electrons in atoms²¹) one can additionally neglect the off diagonal elements of the spin-orbit operator (\mathbf{LS}). The fine structure of the electron level with orbital momentum l is described by:

$$E_{l,l_z,s_z} = E_l + \frac{2s_z l_z}{2l+1}\Delta_c(E_l) + \mu_B s_z g_s(E_l, l_z) H + \mu_B l_z \bar{g}_l(E_l) H, \quad (54)$$

where $l_z = -l, \dots, 0, \dots, l$ and $s_z = \pm 1/2$ are the projection of the electron angular momentum and spin on the magnetic field direction and

$$g_s(E_l, l_z) = \bar{g}_s(E_l) + \frac{l^2 + l + l_z^2 - 1}{(2l+3)(2l-1)}\Sigma_{sur}(E_l). \quad (55)$$

Thus the structures of the excited QSLs with $l \geq 1$ may be different in weak and strong magnetic fields and undertake the anticrossing in the intermediate magnetic field (similar to those known for atoms²¹). In nanocrystals the weak, intermediate and strong field regimes depend strongly on the nanocrystal size as well as on its surface conditions.

V. DISCUSSION AND CONCLUSION

We have studied the effect of general boundary conditions (the surface effect) on the electron QSLs and their Zeeman splitting in spherical bare semiconductor nanocrystals. The above consideration that has been carried on in the eight-band effective mass model can be easily extended to describe spherically layered heterostructures and wide gap semiconductor nanocrystals, which are better described by the fourteen-band model (see for example Ref. 38).

Comparing the results of our theoretical calculation with the experimental size dependence of the electron g -factor we have determined the surface parameter $Ta_0 = -0.6 \pm 0.05 \text{ \AA}$ in bare CdSe nanocrystals. Fitting the experimental data, we used $E_p = 19.0 \text{ eV}$, that has been obtained independently from bulk measurements³⁵ and that describes better the experimental data than $E_p = 17.5 \text{ eV}$, previously used for CdSe in Refs. 4,5. The surface parameter Ta_0 characterizes the electronic properties of the surface and should be considered as the additional one to the set of parameters that describes the bulk properties of semiconductors. In CdSe nanocrystals prepared by a different technique Ta_0 can be different.

The extracted absolute value and the negative sign of $Ta_0 = -0.6 \text{ \AA}$ is consistent with our theoretical expectations for Ta_0 in studied CdSe nanocrystals. Its value is very close to the theoretical value of the surface parameter for semiconductors with a symmetrical band structure²⁶ $|(Ta_0)_s| \equiv a^* = \sqrt{\hbar^2/2E_p m_0} \approx 0.45 \text{ \AA}$. It can also be shown within the eight band effective mass model, that the negative sign of the surface parameter does not allow the existence of the surface localized states with $E < 0$ (gap states) (one can find similar consideration in Ref. 26). Indeed, the CdSe samples studied in Refs. 12,13 show very high PL quantum efficiency and do not show deep gap transitions. The negative parameter Ta_0 leads also to an additional nonparabolicity, bowing the size dependence of the electron energy levels (see Fig. 1) and therefore may describe the unexplained experimental size dependence of the 1S electron level in small CdSe nanocrystals.⁵

Using the GBCs we have found also the direct surface contribution to the spin-orbit effects in zero and weak external magnetic fields. The surface contribution to the zero field spin-orbit splitting is similar to the interface contribution obtained in Refs. 39,40 for 2D electrons in planar quantum wells by using the spin-dependent boundary conditions. It has been pointed out in Ref. 39 that the interface contribution to the Rashba spin-orbit term in the 2D Hamiltonian⁴¹ is related to discontinuity of the band parameters at the semiconductor heterointerface and that this contribution is an additional one to those connected with the space charge and/or the external electric field. The importance of the effects described by the Rashba term for the 2D electrons confined near the curved surface^{42,43} and cylindrical semiconduc-

tor quantum dots⁴⁴ has been emphasized recently. The Rashba spin-orbit term in our spherical dots is a direct consequence of the GBCs for the envelope function. The same consideration can be made for cylindrical dots or any other nanostructure geometry (the results will be published elsewhere). The GBCs provide an important connection between the constant that describes the magnitude of the spin-orbit term and surface conditions in nanostructures.

In conclusion, we have shown an important influence of the semiconductor surface on the electron energy structure in bare spherical nanocrystals. The effect of the surface has been modeled through the choice of the boundary condition parameter that describes the nonzero value of the envelope function at the nanocrystal surface. The additional nonparabolicity of the quantum size energy levels, the spin-orbit splitting of the electron quantum size levels, and the additional magnetic moment of the electrons have been shown to be induced by the surface. The effects are significant in small nanocrystals and their considerations require a multiband effective mass approach because interband coupling is important there. The analysis of the experimental data allows us to determine the appropriate parameter of the boundary conditions that characterize the surface in studied bare CdSe semiconductor nanocrystals.

Acknowledgments

The authors thank I. A. Merkulov and B. K. Meyer for helpful discussions and J. Tischler for a critical reading of the manuscript. The work of A. V. Rodina was supported in part by the Alexander von Humboldt Foundation, Deutsche Forschungsgemeinschaft (DFG) and the Swiss National Science Foundation. Al. L. Efros thanks the U.S. Office of Naval Research (ONR), U.S. Department of Energy (DOE), and the DARPA/QuIST program for financial support. A. Yu. Alekseev acknowledges support from the Swiss National Science Foundation and of the grant of INTAS 99-1705.

APPENDIX: EFFECT OF THE SMALL SURFACE PERTURBATION ON THE QUANTUM SIZE LEVEL ENERGY IN SPHERICAL NANOCRYSTALS

We are interested in deriving a variation of the electron level energy E caused by a small variation of the parameter ς that characterizes the surface BC for the bulk wave function $f(r, \varsigma)$. The GBCs at the spherical surface of the nanocrystal with radius $r = a$ can be written as

$$f'(a, \varsigma) = f(a, \varsigma)A(\varsigma), \quad (\text{A.1})$$

where $A(\varsigma)$ is the real number constant. The function $f(r, \varsigma)$ is the solution of bulk Schrödinger equation

$D\hat{k}^2 f(r, \varsigma) = E(\varsigma)f(r, \varsigma)$ where the constant D is independent of ς . Taking a derivative of the Schrödinger equation on ς , multiplying both parts of the resulting equation by f^* and integrating it over the sphere volume, one can obtain:

$$\frac{\partial E}{\partial \varsigma} = Da^2 \left(\frac{\partial f}{\partial \varsigma} f'^* - \frac{\partial f'}{\partial \varsigma} f^* \right) \Big|_{r=a}. \quad (\text{A.2})$$

Taking a derivative of Eq. (A.1) and substituting $\partial f'(a, \varsigma)/\partial \varsigma = \partial A(\varsigma)/\partial \varsigma f(a, \varsigma) + A(\varsigma)\partial f(a, \varsigma)/\partial \varsigma$ into Eq. (A.2) one arrives at the final expression for the en-

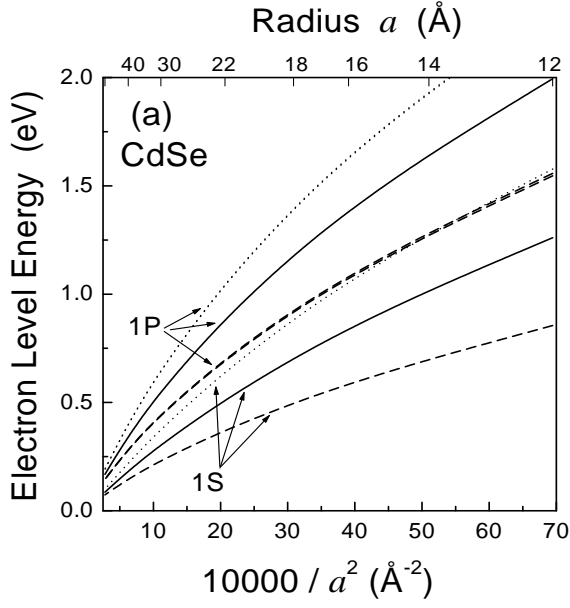
ergy variation:

$$\frac{\partial E}{\partial \varsigma} = -D \frac{\partial A(\varsigma)}{\partial \varsigma} |f(a)|^2 a^2. \quad (\text{A.3})$$

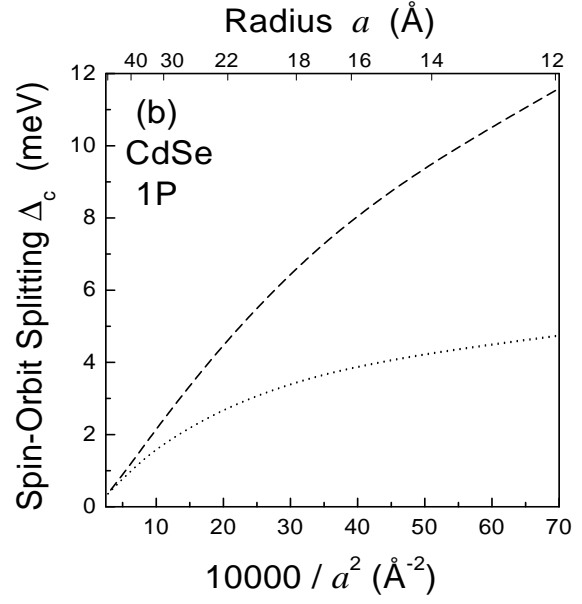
Substituting $D = \hbar^2/2m_c(E_l)$ and $A(\varsigma) = m_c(E_l)/m_0 [1/(Ta_0) + \varsigma]$ with $\varsigma = -\delta k_l^\pm(E_l)$ into this equation we obtain Eq. (33) for the energy correction ΔE_l^\pm to the averaged energy of the electron level with the orbital momentum l caused by the small perturbation of the boundary conditions of Eq. (29).

-
- * On leave from A. F. Ioffe Physico-Technical Institute, 194021, St.-Petersburg, Russia.
- ¹ L. E. Brus, J. Chem. Phys. **79**, 5566 (1983).
 - ² C. B. Murray, D. B. Norris, and M. G. Bawendi, J. Am. Chem. Soc. **115**, 8706 (1993).
 - ³ M. S. Shim and P. Guyot-Sionest, Letters to Nature **407**, 981 (2000).
 - ⁴ A. I. Ekimov, F. Hache, M. C. Schanne-Klein, D. Ricard, C. Flytzanis, I. A. Kudryavtsev, T. V. Yazeva, A. V. Rodina and Al. L. Efros, J. Opt. Soc. Am. B **10**, 100 (1993).
 - ⁵ D. J. Norris and M. G. Bawendi, Phys. Rev. B **53**, 16338 (1996).
 - ⁶ V. I. Klimov, A. A. Mikhailovsky, Su Xu, A. Malko, J. A. Hollingsworth, C. A. Leatherdale, H.-J. Eisler, and M. G. Bawendi, Science **290**, 314 (2000).
 - ⁷ U. Banin, Y. W. Cao, D. Katz, and O. Millo, Letters to Nature **400**, 542 (1999); O. Millo, D. Katz, Y. W. Cao, and U. Banin, Phys. Rev. B **61**, 16773 (2000).
 - ⁸ B. Alpers, I. Rubinshtein, G. Hodes, D. Porath, and O. Millo, Appl. Phys. Lett. **57**, 1751 (1999).
 - ⁹ P. Guyot-Sionest, M. Hines, Appl. Phys. Lett. **72**, 686 (1998); P. Guyot-Sionest, M. Shim, C. Matranga, and M. Hines, Phys. Rev. B **60**, R2181 (1999).
 - ¹⁰ M. Kuno, M. Nirmal, M. G. Bawendi, Al. L. Efros, and M. Rosen, J. of Chem. Phys. **108**, 4242 (1998).
 - ¹¹ A. A. Sirenko, V. I. Belitsky, T. Ruf, M. Cardona, A. I. Ekimov, and C. Trallero-Giner, Phys. Rev. B **58**, 2077 (1998).
 - ¹² J. A. Gupta, D. D. Awschalom, X. Peng, and A. P. Alivisatos, Phys. Rev. B **59**, R10421 (1999).
 - ¹³ J. A. Gupta, D. D. Awschalom, Al. L. Efros, and A. V. Rodina, Phys. Rev. B **66**, 125307 (2002).
 - ¹⁴ O. I. Mičić, A. J. Nozik, E. Lifshitz, T. Rajh, O. G. Poluektov, and M. C. Thurnauer, J. Phys. Chem. B **106**, 4390 (2002).
 - ¹⁵ L. Langof, E. Ehrenfreund, E. Lifshitz, O. I. Mičić, and A. J. Nozik, J. Phys. Chem. B **106**, 1606 (2002).
 - ¹⁶ E. Lifshitz, H. Porteau, A. Glozman, H. Weller, M. Pfughoefft, and A. Eychmüller, J. Phys. Chem. **103**, 6870 (1999).
 - ¹⁷ Al. L. Efros, M. Rosen, M. Kuno, M. Nirmal, D. J. Norris, and M. Bawendi, Phys. Rev. B **54**, 4843 (1996).
 - ¹⁸ A. P. Alivisatos, Science **271**, 933 (1996).
 - ¹⁹ A. Hasselbarth, A. Eychmüller, R. Eichberger, M. Gierzig, A. Mews, H. Weller, J. Phys. Chem. **97**, 5333, 1993; H. Weller, Adv. Matter. **5**, 88 (1993); D. Schooss, A. Mews, A. Eychmüller, H. Weller, Phys. Rev. **B** **49**, 17072 (1994); A. Mews, A. V. Kadavanich, U. Banin, and A. P. Alivisatos, Phys. Rev. B **53**, R13242 (1996).
 - ²⁰ M. Kuno, J. K. Lee, B. O. Dabbousi, F. V. Mikulec, M. G. Bawendi, J. Chem. Phys. **106**, 9869 (1997); S. A. Empeccoles, D. J. Norris, M. G. Bawendi, Phys. Rev. Lett. **77**, 3873 (1996).
 - ²¹ H. A. Bethe and E. E. Salpiter, *Quantum Mechanics of One and Two Electron Atoms*, Springer, Berlin, 1957.
 - ²² L. M. Roth, B. Lax, and S. Zwerdling, Phys. Rev. **114**, 90 (1959).
 - ²³ C. Hermann and C. Weisbuch, Phys. Rev. B **15**, 823 (1977).
 - ²⁴ A. A. Kiselev, E. L. Ivchenko and U. Rössler, Phys. Rev. B **58**, 16353 (1998); E. L. Ivchenko and A. A. Kiselev, JETP Lett. **67**, 43 (1998).
 - ²⁵ L. S. Braginsky, Phys. Rev. B **60**, R13970 (1999).
 - ²⁶ A. V. Rodina, A. Yu. Alekseev, Al. L. Efros, M. Rosen, and B. K. Meyer, Phys. Rev. B **65**, 125302 (2002).
 - ²⁷ A. Abragam and J. H. Van Vleck, Phys. Rev. **92**, 1448 (1953).
 - ²⁸ H. Margenau, Phys. Rev. **57**, 383 (1940).
 - ²⁹ C. R. Pidgeon and R. N. Brown, Phys. Rev. **146**, 575 (1966).
 - ³⁰ G. L. Bir and G. E. Pikus, *Symmetry and Strain-Induced Effects in Semiconductors* (Wiley, New York, 1974).
 - ³¹ E. L. Ivchenko and G. E. Pikus, *Superlattices and Other Heterostructures* (Springer, Berlin, 1995).
 - ³² J. M. Luttinger, Phys. Rev., **102**, 1030, (1956).
 - ³³ G. Dresselhaus, A. F. Kip, and C. Kittel, Phys. Rev. **98**, 368 (1955).
 - ³⁴ L. D. Landau and E. M. Lifshitz, *Quantum Mechanics* (Pergamon Press, N. Y. 1989).
 - ³⁵ A. V. Kapustina, B. V. Petrov, A. V. Rodina, and R. P. Seisyan, Fiz. Tverd. Tela **42**, 1207 (2000) [Phys. Sol. State **42**, 1242 (2000)].
 - ³⁶ *Semiconductors. Physics of II-VI and I-VII Compounds, Semimagnetic Semiconductors*, edited by K.H. Hellewege, Landoldt-Börnstein, New Series, Group III, Vol. 17 b (Springer Verlag, Berlin, 1982).
 - ³⁷ In Ref. 38 we have mistakenly associated this term with the surface contribution to the orbital Zeeman effect.
 - ³⁸ A. V. Rodina, Al. L. Efros, M. Rosen, and B. K. Meyer, Material Science and Engineering C **19**, 435 (2002).
 - ³⁹ E. A. de Andrada e Silva, G. C. La Rocca, and F. Bassani, Phys. Rev. B **55**, 16293 (1997).
 - ⁴⁰ F. T. Vasko, Pis'ma Zh. Eksp. Teor. Fiz. **30**, 574 (1979)

- [JETP Lett. **30**, 541 (1979)].
- ⁴¹ Yu. A. Bychkov and E. I. Rashba, Pis'ma Zh. Eksp. Teor. Fiz. **39**, 66 (1984) [JETP Lett. **39**, 78 (1984)]; J. Phys. C **17**, 6039 (1984).
- ⁴² M. V. Entin and L. I. Magarill, Phys. Rev. B **64**, 085330 (2001).
- ⁴³ L. I. Magarill, D. A. Romanov, and A. V. Chaplik, Pis'ma Zh. Eksp. Teor. Fiz. **64**, 421 (1996) [JETP Lett. **64**, 460 (1996)].
- ⁴⁴ O. Voskoboynikov, C. P. Lee, and O. Tretyak, Phys. Rev. B **63**, 165306 (2001).

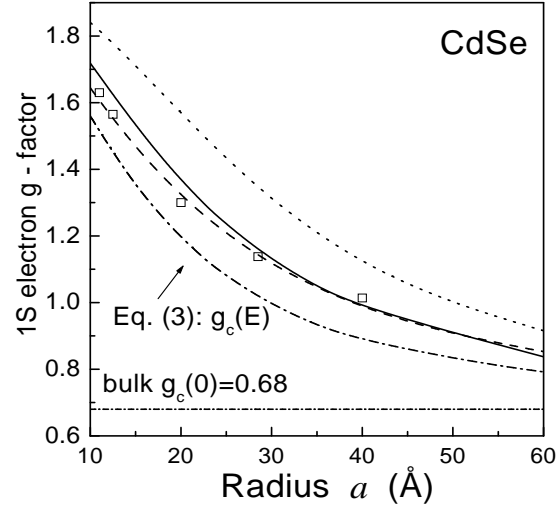


Rodina et al.: Fig. 1(a)



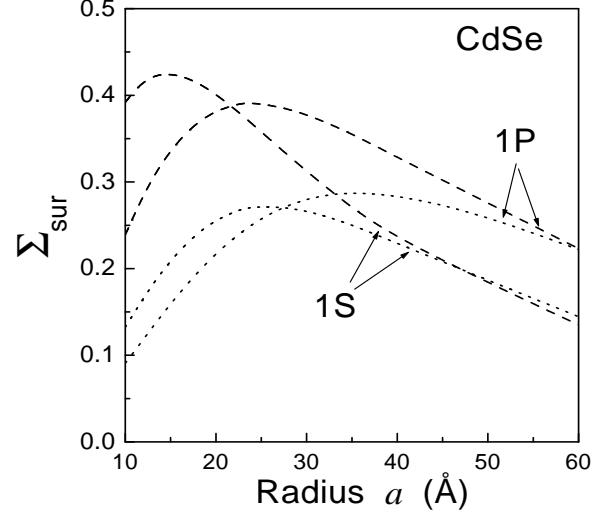
Rodina et al.: Fig. 1(b)

FIG. 1: The effect of general boundary conditions on the ground $1S$ and first excited $1P$ energy levels (a), and on the spin-orbit splitting between $1P_{3/2}$ and $1P_{1/2}$ levels Δ_c (b) in bare CdSe nanocrystals. The size dependencies are calculated for the standard BCs with the surface parameter $Ta_0 = 0 \text{ \AA}$ (solid line), for $Ta_0 = -0.6 \text{ \AA}$ (dashed lines), and for $Ta_0 = 0.6 \text{ \AA}$ (dotted lines). The bulk parameters of CdSe used in calculations are described in the text.



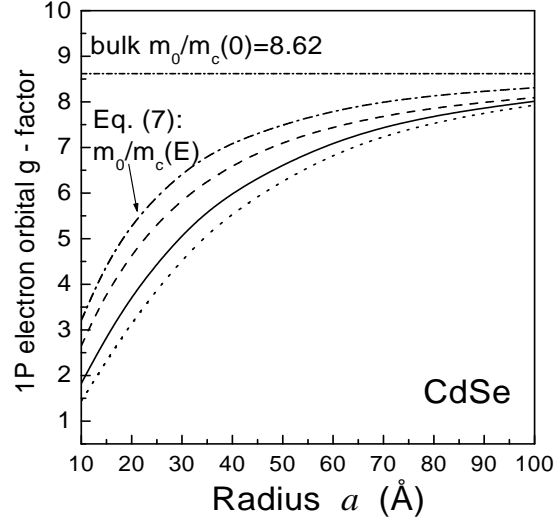
Rodina et al.: Fig. 2

FIG. 2: The size dependence of the ground $1S$ state electron g -factor in bare CdSe nanocrystals calculated for the standard BCs with the surface parameter $Ta_0 = 0$ (solid line), for $Ta_0 = -0.6 \text{ \AA}$ (dashed line), and for $Ta_0 = 0.6 \text{ \AA}$ (dotted line). The empty squares show the experimental data from Ref. 13. For comparison we also show the energy dependence of the bulk electron g -factor $g_c(E)$ calculated at the energy of the $1S$ electron level (dash-dotted line) and bulk value of the electron g -factor (short dash-dotted line).



Rodina et al.: Fig. 3

FIG. 3: The size dependence of the dimensionless surface parameter Σ_{sur} of Eq. (37) for the ground 1S ($l = 0$) and first excited 1P ($l = 1$) states in bare CdSe nanocrystals. The dashed and dotted curves are calculated with the surface parameters $Ta_0 = -0.6 \text{ \AA}$ and $Ta_0 = 0.6 \text{ \AA}$ respectively.



Rodina et al.: Fig. 4

FIG. 4: The size dependence of the orbital g -factor, $\bar{g}_l(1P)$, for the first excited state in bare CdSe nanocrystals calculated for the standard BCs with surface parameter $Ta_0 = 0$ (solid line), for $Ta_0 = -0.6 \text{ \AA}$ (dashed lines), and for $Ta_0 = 0.6 \text{ \AA}$ (dotted lines). For comparison we also show the bulk energy dependence of the bulk orbital g -factor $m_0/m_c(E)$ calculated at the energy of the $1P$ electron level (dash-dotted line) and its value at the bottom of the conduction band (short dash-dotted line).